

Synthesis and magnetic properties of $\text{Fe}_{51}\text{Pt}_{27}\text{Nb}_2\text{B}_{20}$ melt spun ribbons

A. D. CRISAN, O. CRISAN, I. SKORVANEK^a, N. RANDRIANANTOANDRO^b

National Institute for Materials Physics, P.O. Box MG-7, 077125 Bucharest-Magurele, Romania

^aInstitute of Experimental Physics, Slovak Academy of Sciences, 040-01 Kosice, Slovakia

^bLaboratoire de Physique de l'Etat Condense, UMR 6034 CNRS, Universite du Maine, 72000 Le Mans, France

Fe-Pt alloys have gained much interest for the occurrence of permanent magnetic features resulting from the L_{10} ordered face-centred-tetragonal FePt phase with very high magnetic crystalline anisotropy ($7 \times 10^6 \text{ J/m}^3$). An amorphous melt spun ribbons of the composition $\text{Fe}_{51}\text{Pt}_{27}\text{Nb}_2\text{B}_{20}$ has been synthesized by the rapid solidification technique and its microstructure and magnetic properties were studied. After appropriate annealing, an ordered face-centred-tetragonal (f.c.t.) L_{10} phase is formed. X-ray analysis revealed a structural phase transformation from the body-centered-cubic A1 to f.c.t. L_{10} phase and this produce magnetic hardening of the alloy, upon appropriate annealing conditions. Extremely performant magnetic properties, typical for exchange spring magnets, are obtained.

(Received February 25, 2008; accepted April 2, 2008)

Keywords: Structural phase transformations, Fe-Pt alloys, Nanocomposite magnets, Melt spun ribbons, Fe-Pt-Nb-B

1. Introduction

In the last years nanocomposite magnets have attracted considerable attention due to several technological applications [1-3]. Nanocomposite magnets are composed of magnetically hard and soft phases on a nanometric scale that are suitably and alternatively disposed within a homogeneous microstructure and interact via magnetic exchange coupling mechanisms. The hard magnetic phase has high anisotropy and high coercive fields and the soft phase has enhanced saturation magnetization.

Strong exchange coupling between the hard and soft phases gives rise to further enhancement in remanence, coercivity and maximum energy product. The magnetic properties of the nanocomposite magnets are strongly dependent on the microstructure and intrinsic alternate disposal of soft and hard magnetic regions. Different techniques, such as: mechanical milling, casting, self-assembly, sputtering and melt spinning have been used to prepare exchange spring magnets.

The melt spinning technique has some advantages: requires a small quantity of materials, it is fast and reliable process, with reduced costs compared with other techniques, and gives completely reproducible results. Also, it is very useful because the amorphous structure of the as-obtained ribbons can be easily transformed into nano-sized crystalline grains by subsequent heat treatments.

The interest for FePt based alloys increased recently due to their outstanding potential for technological applications as, for example, magnetic recording media, magnetic field sensors, and exchange spring magnets. In the form of nanocrystalline alloys, these nanocomposite spring magnets have high corrosion resistance and exhibit, upon appropriate annealing, the ordered hard magnetic tetragonal L_{10} FePt phase with a large magnetocrystalline anisotropy ($7 \times 10^6 \text{ MJ/m}^3$). Pt exhibits strong affinity to Fe in forming

magnetically hard L_{10} phase during thermal annealing. The addition of B allows the formation of amorphous as-cast state and Nb was added in order to limit the grain growth during annealing treatments. In this study, we focus on the magnetic and crystalline microstructure of melt spun $\text{Fe}_{51}\text{Pt}_{27}\text{Nb}_2\text{B}_{20}$.

2. Experimental

The $\text{Fe}_{51}\text{Pt}_{27}\text{Nb}_2\text{B}_{20}$ sample was prepared by melt spinning technique in Ar controlled atmosphere. The purity of all the starting elements was 99.95%. The primary alloy was melted three times in arc furnace, purged onto the Cu wheel and rapidly solidified during the high speed wheel rotation with a 10^6 K/min cooling rate.

The analysis of the crystal structure of sample and the phase composition was examined by X-ray diffraction (XRD) using a Bruker G8 diffractometer with Cu $K\alpha$ radiation. The mean grain size was derived from the peak broadening of XRD lines using Scherrer's formula. The phase transformation was studied by differential scanning calorimetry (DSC) using Netzsch DSC 4 facility in vacuum (10^{-3} torr). During the DSC process, the sample was heated up to $700 \text{ }^\circ\text{C}$ with a 5 K/min heating rate. The magnetic measurements were done at room temperature with an Oxford Instruments superconducting quantum interference device (SQUID), with the applied field up to 5 Tesla, parallel to the ribbons plane. Annealing of the as-cast sample has been done at $500 \text{ }^\circ\text{C}$ for 30 minutes followed by another 30 minutes at $600 \text{ }^\circ\text{C}$. Other annealings were performed at $700 \text{ }^\circ\text{C}$ for 40 minutes and 2 hours respectively. The annealings were done in an inductive furnace with strict control of the temperature ($\pm 2^\circ\text{C}$) under Ar atmosphere.

3. Results and discussion

The initial alloy, as obtained from the melt spinning facility, has been checked by XRD in order to observe the as-cast state of the obtained ribbons. It has been observed that the as-cast state is mainly amorphous, with small nucleation sites that acted as nanocrystals.

In order to observe the crystallization process and the cubic-to-tetragonal structural phase transformation, to monitor its temperature and energy of formation, thermal analysis has been performed using the DSC facility. As the as-cast state is mainly amorphous, it is of crucial interest to obtain information regarding the crystallization process, such as: the temperature of crystallization and the energy associated to the primary crystallization process, the crystallization kinetics and whether it occurs in multiple steps, the type of crystallization process (primary, polymorphic) and so on.

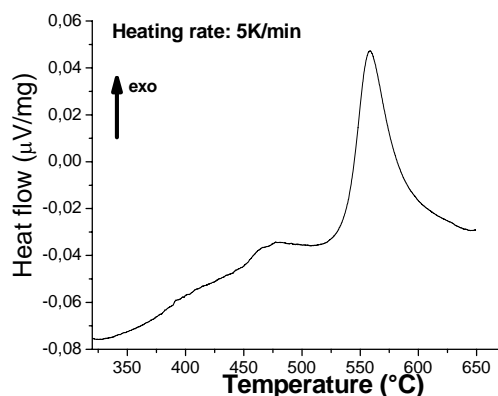


Fig. 1. DSC scan of the as-cast sample recorded upon heating from RT up to 670 °C, with 5K/min heating rate.

Fig. 1 presents the DSC scan recorded between room temperature and 670 °C, at a heating rate of 5K/min. The slowest possible heating rate has been chosen in order to carefully detect both the crystallization temperature and the true onset of the eventual exothermic events that may correspond to the structural cubic-tetragonal phase transformation. Since this is normally a disorder-order phase transition, it should occur by emanating specific heat to the exterior, therefore it must be observed in the DSC scan as a strong exothermic event.

At low temperatures, i.e. below 520 °C, the scan is showing quite linear dependence, with some small kinks and exothermic effects, mostly related to the interphase atomic diffusion and to the relaxation of thermal stresses induced in ribbons during the rapid solidification synthesis procedure. A strong, well-defined, exothermic peak, characteristic for amorphous ribbons, occurs at around 570 °C. The peak with typical Lorentzian shape is most probably related to the primary crystallization of the sample. As there is only one main peak with single Lorentzian line profile, assigned to the primary crystallization of the sample, until the maximum of the investigated temperature

(670 °C) it seems that the polymorphic crystallization as well as the exothermic events related to the coarsening of the microstructure, occurs only after this temperature. As was previously pointed out in alloys with similar composition [4], the cubic-to-tetragonal FePt structural phase transformation occurs almost simultaneously with the primary crystallization. Therefore the area encompassed by the main exothermic peak corresponds to the energy of primary crystallization process summated with the energy of the system exchanged with the outer space during the structural phase transformation. Both are disorder-order phase transitions and occur by emanating energy to the exterior, being observed as exothermic effects in the DSC scan. A study of the crystallization kinetics through Johnson-Mehl-Avrami model is actually in progress.

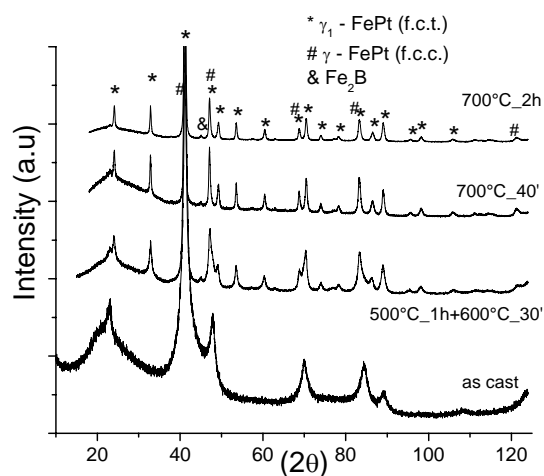


Fig. 2. XRD spectra of as-cast and annealed samples. The observed Bragg peaks are indexed on the figure and corresponds mainly to $L1_0$ FePt (or γ_1 f.c.t.), $A1$ FePt (or γ f.c.c.) and Fe_2B .

As mentioned above, three different annealing procedures were performed, and the corresponding samples were checked by XRD. Fig. 2 shows the X-ray spectra of as-cast and annealed samples. It can be observed that the spectra of annealed samples exhibit sharp Bragg peaks, indicating the high degree of crystallinity in these samples. On the contrary, the as-cast state was found to be mainly a mixture of an amorphous state with a nanocrystalline solid solution of apparently cubic symmetry, as proven by the very broad lines in the diffraction spectrum and the indexation of their Bragg reflections that correspond mainly to the f.c.c. cubic FePt-rich solid solution. As the samples are annealed, the microstructure evolves into refining the width of the Bragg reflections, kept at the same angular position. This result proves that the incipient nucleation sites with a cubic symmetry from the as-cast state, evolve into larger nanocrystals but keeping the same crystal symmetry. The width of the Bragg peaks is highly reduced which indicates the onset of the crystallization process in the 500/600 °C heated sample, and the decrease of the Bragg peaks width is more pronounced for the two

samples annealed at 700 °C. The indexation of the diffraction lines for the annealed samples provides the image of some complex phase composition in these samples. The main phases that are indexed in the XRD spectra of annealed samples are mainly the f.c.t. $L1_0$ FePt and f.c.c. A1 FePt, together with small amount of boride, formed in later stages of annealing by polymorphic crystallization of the remaining amorphous phase. Since it is quite difficult to distinguish between the diffraction lines of the ordered tetragonal $L1_0$ and disordered cubic A1 FePt, a Rietveld-type refinement technique needed to be used in order to correctly index the observed peaks. We have been able to determine the lattice parameters of tetragonal $L1_0$ (S.G. $P4/mmm$) and f.c.c. A1 (S.G. $Fm\bar{3}m$), values that are listed in Table I. It can be seen that the lattice parameters globally decreases with increasing the temperature and time of annealing. This is in line with the hypothesis of refining the lattice by segregating the substitutional atoms, that in the as-cast state, form the initial cubic solid solution. Also, the tetragonal FePt phase follows the same trend. It proves that the microstructure is refined and foreign atoms (eg. Nb and B) are gradually expelled towards the grain boundaries upon increasing the annealing temperature and the annealing time. The average crystallite size was determined by Scherrer's formula, corrected for instrumental broadening. The results shown in Table 1 as well, give an image of the very uniform nanocrystalline microstructure in the as-cast state, with small nucleation sites and nanocrystals with an average size of 4.2 nm. Upon annealing, the grain size increases, since both tetragonal FePt and cubic FePt crystallizes from the initial solid solution. But the values, even at annealing temperatures as high as 700°C and for annealing times as great as 2 hours, are still below or around 15 nm. Nb added in the initial alloy as an element that was meant to stop the grain growth in secondary stages of annealing, has been proven to be very effective in our case, for this purpose. This shows that upon annealing the microstructure is formed by small enough grain so that the requirements for an exchange spring magnets to be fulfilled. It has to be mentioned that for an effective exchange coupling between hard tetragonal FePt grains and soft cubic FePt ones, the grain sizes must not exceed the exchange correlation length and they must be in a monodomainal state from the magnetic point of view. More detailed analysis is though required in order to provide a more accurate refinement of the X-ray spectra, for taking into account also the presence of possible Fe-B-rich amorphous regions, visible in the XRD spectrum of the as-cast sample.

Table I. Lattice parameters from Rietveld-type refinement of the XRD spectra and average grain sizes for each identified phase as resulted from evaluations with Scherrer's formula, for the as-cast and annealed samples.

Parameters	Cubic FePt		Tetragonal FePt		
	Grain size (nm)	Lattice constant a (Å)	Grain size (nm)	Lattice constant a (Å)	Lattice constant c (Å)
As-cast	4.2	3.789	-	-	-
500/600°C	9.7	3.772	8.6	3.76	3.786
700°C_40mn	10.2	3.766	13.1	3.752	3.779
700°C_2h	15.1	3.756	14.2	3.746	3.773

The magnetic measurements performed with a superconducting quantum interference device (SQUID) at 5 K and 300 K show outstanding exchange spring behavior for the annealed samples, compared to the as-cast sample that is essentially a soft magnet with high saturation magnetization and virtually no hysteresis. The annealed samples show extremely high coercivity values of 14.5 kOe at 5 K and 11.2 kOe at 300 K, that are comparable with the best exchange spring magnets reported in the literature and important values of the remanent magnetization, which gives an extremely elevated energy product that makes the signature of a very performant exchange spring magnet.

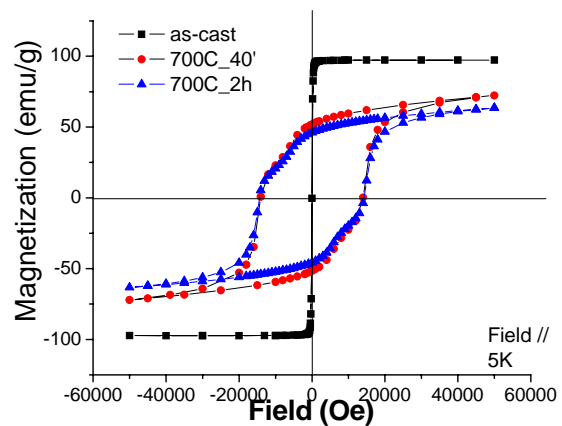


Fig. 3. Hysteresis loops at 5K recorded for as-cast and annealed samples in parallel applied field.

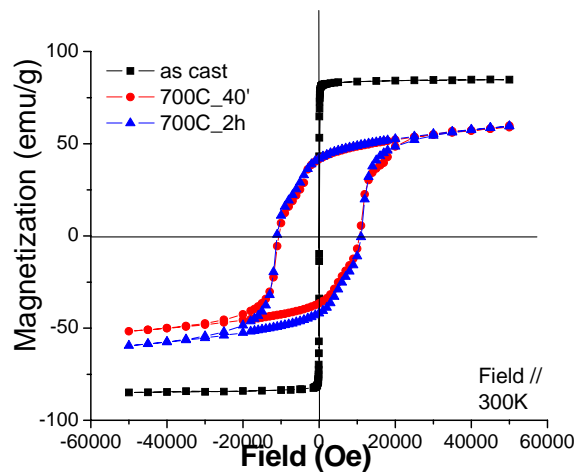


Fig. 4. Hysteresis loops at 300K recorded for as-cast and annealed samples in parallel applied field.

The inflection points observed in the annealed samples loops at around 3.8 and 9.8 kOe in the 300 K loops represent the reversal fields of the soft phases, Fe_2B and cubic FePt. Nevertheless, the existence of such inflection point as well as the shape of the loops indicates that the hard and soft phases are not fully exchange coupled. This indicates that it is possible to obtain even more increased coercivity and energy product if the regular disposal of hard

and soft grains would allow an intimately, fully coupled exchange between them. We give thus further evidence of the co-existence of soft and hard magnetic phases in our annealed samples, in a refined grain microstructural arrangement that allows one to obtain such promising magnetic properties, compatible with performant exchange spring magnets.

5. Conclusions

An amorphous melt spun ribbons of the composition Fe₅₁Pt₂₇Nb₂B₂₀ has been synthesized by the rapid solidification technique and its microstructure and magnetic properties were studied. After appropriate annealing, an ordered face-centred-tetragonal (f.c.t.) L1₀ phase is formed. X-ray analysis revealed the co-existence of the soft magnetic body-centered-cubic A1 with hard magnetic f.c.t. L1₀ FePt phase and this produce magnetic hardening of the alloy, upon appropriate annealing conditions. The annealed samples show co-existence of hard and soft magnetic phase, a two-phase behavior accompanied with a well-refined grain microstructure. These features are the key issues for the extremely high coercivity values that we have obtained here, values that are comparable with the best exchange spring magnets reported in the literature.

Acknowledgements

The authors acknowledge the help of Dr. I. Skorvanek for the magnetic measurements. The work has been performed with the financial support in the frame of the Excemag network of excellence, project CEEX 20/2005 of the Romanian Ministry of Education and Research, as well as in the frame of bilateral cooperation agreement between CNRS-France and Romanian Academy.

References

- [1] T. Nagahama, K. Mibu, T. Shino, J. Phys. D **31**, 43 (1998).
- [2] W. Liu, Z. A. Zhang, J. P. Liu, J. J. Chen, L. L. He, Y. Liu, X. K. Sun, D. J. Sellmyer, Adv. Mater. **14**, 1832 (2002).
- [3] X. Ruj, E Shield, Z. Sun, Y. Xu, D. J. Sellmyer, Appl. Phys. Lett. **89**, 122509 (2006).
- [4] O. Crisan, A. D. Crisan, N. Randrianantoandro, R. Nicula, E. Burkel, J. Alloys & Comp. **440**, L3-L7 (2007).

*Corresponding author: ocrisan@yahoo.com